THE JOURNAL OF BIOLOGICAL CHEMISTRY VOL. 286, NO. 52, pp. 45063–45072, December 30, 2011

Translational Repression of the Disintegrin and Metalloprotease ADAM10 by a Stable G-quadruplex Secondary Structure in Its 5′-Untranslated Region*[S]

Received for publication, August 23, 2011, and in revised form, November 3, 2011 Published, JBC Papers in Press, November 7, 2011, DOI 10.1074/jbc.M111.296921

Sven Lammich[‡1], Frits Kamp[‡], Judith Wagner[‡], Brigitte Nuscher[‡], Sonja Zilow[‡], Ann-Katrin Ludwig[‡], Michael Willem[‡], and Christian Haass[‡§2]

From the [‡]Adolf Butenandt Institute, Biochemistry, Ludwig Maximilians University, 80336 Munich, Germany and [§]DZNE (German Center for Neurodegenerative Diseases), 80336 Munich, Germany

Background: Translation of the α-secretase ADAM10 is repressed by its 5′-untranslated region (5′-UTR).
Results: A G-rich region in the *ADAM10* 5′-UTR forms a highly stable G-quadruplex secondary structure, which inhibits translation of a luciferase reporter and ADAM10.
Conclusion: The G-quadruplex secondary structure is one inhibitory element for ADAM10 translation.
Significance: Our findings provide new insights in the translational regulation of ADAM10.

Anti-amyloidogenic processing of the amyloid precursor protein APP by α-secretase prevents formation of the amyloid-β peptide, which accumulates in senile plaques of Alzheimer disease patients. α-Secretase belongs to the family of a disintegrin and metalloproteases (ADAMs), and ADAM10 is the primary candidate for this anti-amyloidogenic activity. We recently demonstrated that ADAM10 translation is repressed by its 5′-UTR and that in particular the first half of *ADAM10* 5′-UTR is responsible for translational repression. Here, we asked whether specific sequence motifs exist in the *ADAM10* 5′-UTR that are able to form complex secondary structures and thus potentially inhibit ADAM10 translation. Using circular dichroism spectroscopy, we demonstrate that a G-rich region between nucleotides 66 and 94 of the *ADAM10* 5′-UTR forms a highly stable, intramolecular, parallel G-quadruplex secondary structure under physiological conditions. Mutation of guanines in this sequence abrogates the formation of the G-quadruplex structure. Although the G-quadruplex structure efficiently inhibits translation of a luciferase reporter in *in vitro* translation assays and in living cells, inhibition of G-quadruplex formation fails to do so. Moreover, expression of ADAM10 was similarly repressed by the G-quadruplex. Mutation of the G-quadruplex motif results in a significant increase of ADAM10 levels and consequently APPsα secretion. Thus, we identified a critical RNA secondary structure within the 5′-UTR, which contributes to the translational repression of ADAM10.

The pathological hallmarks of Alzheimer disease are extracellular amyloid plaques and intracellular neurofibrillary tangles. Amyloid plaques are composed of the amyloid-β peptide, which is liberated via sequential cleavage of the amyloid precursor protein (APP)[3] by β- and γ-secretase (1). Alternatively, α-secretase cleaves APP within its amyloid-β domain and therefore prevents formation of the neurotoxic amyloid-β peptide. α-Secretase cleavage liberates APPsα, which may have neuroprotective and neurotrophic properties (2, 3). The remaining C-terminal fragment of APP is further processed by γ-secretase to produce the non-amyloidogenic fragment p3 (4).

Three members of the large family of disintegrin and metalloproteinases (ADAM) apparently exert α-secretase activity: ADAM9, ADAM10, and ADAM17 (5–7). Among these, ADAM10 is the major candidate for the physiological α-secretase because moderate overexpression of ADAM10 in an Alzheimer disease mouse model resulted in increased APPsα shedding, lowering of amyloid-β peptide generation, and consequently, a reduction of the amyloid plaque load (8). In addition, it was shown recently that siRNA-mediated knockdown of ADAM10 in mammalian cells and primary neurons abolished the generation of APPsα, whereas knockdown of ADAM9 or ADAM17 still allowed robust production of APPsα (9). ADAM10 knock-out mice die at day embryonic day 9.5 of embryogenesis with multiple defects in the developing central nervous system, somite segmentation, and the cardiovascular system, emphasizing an important role of ADAM10 in development (10). To analyze the function of ADAM10 in brain development, neuron-specific ADAM10-deficient mice were generated (11). These mice die perinatally due to a down-regu-

* This work was supported by the Deutsche Forschungsgemeinschaft (Collaborative Research Center (SFB596) "Molecular Mechanisms of Neurodegeneration" (to S. L., M. W., and C. H.)), a fellowship of the Hans and Ilse Breuer Foundation (to S. Z.), the Helmholtz Alliance (Mental Health in an Aging Society, HelMA), the Bundesministerium für Bildung und Forschung ("Degenerative Dementias: Target Identification, Validation, and Translation into Treatment Strategies" (to C. H.)), and by the Center of Integrated Protein Science Munich.
[S] The on-line version of this article (available at http://www.jbc.org) contains supplemental Fig. 1.
[1] To whom correspondence should be addressed: Adolf-Butenandt-Institute, Biochemistry, Schillerstrasse 44, 80336 Munich, Germany. Tel.: 49-89-2180-75484; Fax: 49-89-2180-75415; E-mail: sven.lammich@med.uni-muenchen.de.
[2] Supported by "Forschungsprofessur" of the Ludwig Maximilians University (Munich, Germany).

[3] The abbreviations used are: APP, amyloid precursor protein; IRP, iron-regulatory protein; FMRP, fragile-X mental retardation protein; IRE, iron-responsive element; T_m, melting temperature; ΔH_{vH}, van't Hoff enthalpy; ΔS_{vH}, van't Hoff entropie; ΔG_{vH}, van't Hoff free energy change; Luc, luciferase.

lation of Notch signaling in the brain. However, analysis of APP processing in primary neuronal cultures from embryonic day 14.5 of these conditional ADAM10 knock-out mice revealed a 90% reduction of APPsα generation (11). These data therefore demonstrate that ADAM10 is the predominant α-secretase activity in the brain. Apart from APP and Notch, ADAM10 cleaves other neuronal proteins, like ephrins, L1 adhesion molecule, and N-cadherin, which are important for neurite outgrowth and migration (12, 13). Finally, ADAM10 is up-regulated in several cancers and plays a role in inflammation processes (13).

Regulation of ADAM10 is achieved by multiple mechanisms. ADAM10 is expressed as an inactive prodomain containing zymogene, which is activated by the proprotein convertases furin and PC7 (14). The prodomain is important for folding of ADAM10 and acts as a potent inhibitor of ADAM10 activity (14, 15). Recently, it was demonstrated that *ADAM10* transcription is stimulated by all-trans retinoic acid and by the deacetylase Sirtuin1 (16, 17). Moreover, we demonstrated previously that ADAM10 expression could be suppressed at the translational level by its unusual long GC-rich 5′-UTR (18). Therefore, we hypothesize that the 5′-UTR of *ADAM10* may affect its translation via RNA binding proteins and/or stable RNA secondary structures.

Current knowledge implicates that translational regulation occurs predominantly at the level of initiation and two distinct general modes could be discriminated, global translational regulation, and mRNA-specific regulation (19–21). In general, global control of translation is mediated by phosphorylation of initiation factors (19–21). Translational regulation of specific mRNAs is often achieved by cis-acting elements within UTRs of these mRNAs such as secondary structures, upstream ORFs, internal ribosomal entry sites, and/or trans-acting elements like mRNA binding proteins and microRNAs (19–21). Interestingly, translation of the β-secretase BACE1 is suppressed by its long GC-rich 5′-UTR, which contains several upstream ORFs (22–24). Increased translation of BACE1 was observed in response to energy deprivation, due to increased translation reinitiation at the start codon of the *BACE1* message (25), similar to the translation of yeast GCN4 and ATF4 (26, 27). Moreover, translational repression could be achieved by blocking the recruitment of the preinitiation complex to an mRNA. The best characterized examples for this mechanism are iron-regulatory proteins (IRPs) (28, 29). In iron-deficient cells, IRPs bind to iron-responsive elements (IREs), which form stable stem loops in 5′-UTRs of L- and H-ferritin mRNAs and inhibit translation of these mRNAs (28, 29). An increase of the cellular iron concentration results in dissociation of IRPs from the 5′-UTRs, which leads to increased ferritin mRNA translation (29). More recently, it was hypothesized that RNA G-quadruplex structures within 5′-UTRs are potent translational repressors that block formation or scanning of the preinitiation complex (30). G-quadruplexes are higher-order nucleic acid secondary structures formed by G-rich sequences. The basic structural core motif of G-quadruplexes consists of a series of G-quartet planes, each of which consists of four guanines connected by Hoogsteen-hydrogen bonds and stabilized by monovalent ions, particularly potassium ions (31–34). There is growing evidence that the formation of G-quadruplex secondary structures within 5′-UTRs results in translational repression of a number of different mRNAs, including N-*ras*, *Zic-1*, membrane-type matrix metalloproteinase 3, *ESR-1*, and *Bcl-2* (35–42). Similar to the IRE stem loop, the stability of G-quadruplex structures could be modulated by RNA binding proteins such as FMRP or members of the hnRNP A family (43, 44).

Interestingly, the 5′-UTR of *ADAM10* contains a G-rich sequence between nucleotides 66–94, which, based on a prediction algorithm, may form a stable G-quadruplex secondary structure (see Fig. 1, *A* and *B*). Using CD spectroscopy, we provide evidence that this sequence indeed folds into a stable RNA G-quadruplex *in vitro* and that mutation of several guanines inhibits G-quadruplex formation. The G-quadruplex inhibits a luciferase reporter in cell free lysates and living cells. Moreover, we demonstrate that mutation of the G-quadruplex motif results in increased ADAM10 translation and consequently increased the anti-amyloidogenic processing of APP.

EXPERIMENTAL PROCEDURES

Oligonucleotides—The following RNA oligonucleotides were purchased from Thermo Scientific: ADAM10GQ-WT, UGGGGGACGGGUAGGGGCGGGAGGUAGGGG; ADAM10GQ-mut1, UGGAAGACGAGUAGGAGCGAGAGGUAGGGG; and ADAM10GQ-mut2, UAGAAGACGAAUAGAAGCGAAAAGUAGAAG.

CD Spectroscopy—For spectroscopic studies, RNA oligonucleotides were prepared at 5 μM strand concentration in RNase-free water containing 10 mM Tris/HCl, 0.1 mM EDTA, pH 7.4 in a final volume of 250 μl. The samples were annealed by heating at 90 °C for 10 min and subsequent slow cooling to 20 °C at a constant rate of 0.2 °C/min. CD measurements were performed after a 10-min equilibration at 20 °C using a Jasco J-810 spectropolarimeter equipped with a Peltier temperature cooler in a 0.1-cm cell at a scanning speed of 50 nm/min with a response time of 8 s. The spectra were averaged over 11 scans from 200–320 nm, and data were zero-corrected at 320 nm. For each sample, a buffer baseline was obtained in the same cuvette and subtracted from the average scan.

CD melting curves were recorded as described above in the presence of 1 mM KCl by monitoring ellipticity at 263 nm between 20 and 90 °C. The melting temperature (T_m) was calculated using the van't Hoff method (45).

cDNA Constructs—The *ADAM10* G-quadruplex motif and mutated variants thereof in front of *Renilla* luciferase of the psiCHECK-2 vector (Promega) were generated by PCR using the unique NheI restriction site upstream of the *Renilla* luciferase start codon. pcDNA6/V5-HisA-5′-UTR-Luc with the intact *ADAM10* G-quadruplex motif was described previously (18). Mutated variants of the G-quadruplex motif, 5′-UTR-GQmut1-Luc (TGGAAGACGAGTAGGAGCGAGAGGTAGGGG) and 5′-UTR-GQmut2-Luc (TAGAAGACGAATAGAAGCGAAAAGTAGAAG) were introduced by PCR using appropriate primers. In addition, plasmid pcDNA6/V5HisA-ADAM10 (18), was used to generate GQ-WT ADAM10 and the corresponding mutants GQ-mut1-ADAM10 and GQ-mut2-ADAM10 using NheI/HindIII restriction sites and appropriate primers. All cDNAs were verified by sequencing.

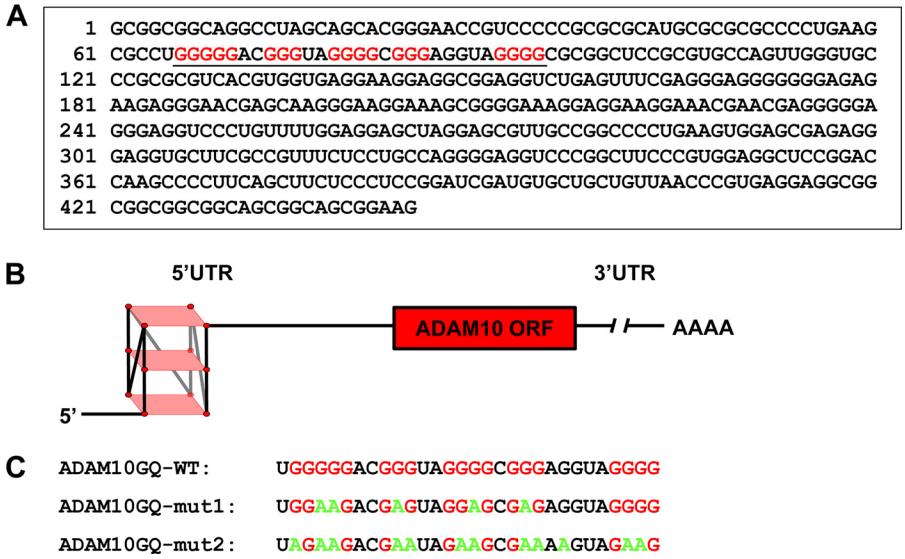

FIGURE 1. **The 5′-UTR of ADAM10 contains a G-quadruplex motif.** *A*, representation of the human ADAM10 5′-UTR-RNA sequence. The predicted G-quadruplex sequence located between nucleotides 66 and 94 of the ADAM10 5′-UTR is *underlined*. The guanines predicted to be involved in the formation of the potential G-quadruplex secondary structure are highlighted in *red*. *B*, model of the parallel ADAM10 5′-UTR G-quadruplex secondary structure. Guanines (*red circles*) of the canonical repeats of the G-rich stretches involved in G-quadruplex formation are located at the four edges of each plane marked in *light red*. *C*, sequences of RNA oligonucleotides used for CD spectroscopy measurements in this study. Guanines potentially involved in G-quadruplex formation are marked in *red*, and substitutions to adenines are highlighted in *green*.

Cell Culture and cDNA Transfections—Human embryonic kidney 293EBNA (HEK293) cells were cultured in DMEM supplemented with 10% fetal bovine serum, 1% penicillin/streptomycin, and 2 mM glutamine. Transfections were carried out using Lipofectamine 2000 (Invitrogen) according to the manufacturer's instructions.

Protein Analysis—1.8×10^6 HEK293 cells were plated in 6-cm dishes and transiently transfected with 8 μg of cDNA encoding ADAM10 variants and 0.1 μg of pEGFP-N1 (Clontech). Protein analysis was performed as described previously (18). For analysis of APP processing, the cell culture medium was replaced 24 h after transfection, and the cells were incubated for 4 h in fresh medium. Equal amounts of conditioned media were analyzed for APPsα using antibody 2D8 (1 μg/ml) (46). Full-length APP was detected using the APP-C-terminal antibody (A8717) from Sigma.

Dual-Luciferase Reporter Assay—1.8×10^5 HEK293 cells were seeded in 24-well plates and transfected with 0.8 μg of psiCHECK-2-GQ-WT, psiCHECK-2-GQ-mut1, or psiCHECK-2-GQ-mut2. 24 h after transfection, cell lysates were prepared, and luciferase activity was measured with the Dual-Luciferase reporter assay system (Promega) according to the manufacturer's instructions. Quantification was performed using an LB96V luminometer (Berthold Technologies) and analyzed with WinGlow software (Berthold Technologies). *Renilla* luciferase activity was normalized to firefly luciferase activity.

Quantitative Real-time PCR—Total RNA was isolated from HEK293 cells 24 h after transfection with psiCHECK-2-GQ plasmids using the RNeasy mini kit (Qiagen), including an on-column DNase digest. Subsequently, the RNA was treated a second time with DNase I (DNA-free, Ambion). cDNA was synthesized from 250 ng of total RNA using MessageSensor RT (Ambion) with random hexamer primers. Quantitative real-time PCR was performed with 2× Power SYBR Green PCR Master Mix (Applied Biosystems) and 0.5 μM of each primer pair (RLuc 344, 5′-TCTTTGTGGGCCACGACTGGGG-3′ (forward primer); RLuc 603, 5′-GGCAGCGAACTCCTCAGGCTCC-3′ (reverse primer); and FLuc 976, 5′-GCCGTGGCCAAGCGCTTTCATC-3′ (forward primer); FLuc 1150, 5′-CTCCCAGGGTCTTGCCGGTGTC-3′ (reverse primer)). ADAM10 mRNA levels were determined as described previously (18). Quantification was performed with the 7500 Fast Real-time PCR system (Applied Biosystems). For each RNA sample, triplicates were analyzed with each primer set, and *Renilla* luciferase RNA expression was normalized to firefly luciferase as described (47).

In Vitro Transcription—Plasmids were linearized using the XhoI restriction enzyme, which cuts at the 3′ end of the coding region of the luciferase reporter gene. 5′-Capped transcripts were generated *in vitro* using the mMESSAGE mMACHINE T7 kit (Ambion), following the manufacturer's instructions. The RNA concentration was determined by UV spectroscopy. The integrity and the size of each transcript were confirmed by 1% agarose gel analysis.

In Vitro Translation—*In vitro* translation of 100 ng of *in vitro*-transcribed mRNAs was carried out in a cell-free translation system consisting of extracts from nuclease-treated rabbit reticulocyte lysate (Promega) as described (48). Firefly luciferase activity was measured in duplicate as described above.

RESULTS

The 5′-UTR of ADAM10 Contains a G-rich Region, which Forms a Stable G-quadruplex Secondary Structure—Using the G-quadruplex secondary prediction algorithm Quadfinder (49), we identified a potential G-quadruplex motif between nucleotide 66 and 94 of the human *ADAM10* 5′-UTR (Fig. 1, *A* and *B*). This G-quadruplex motif is evolutionary conserved

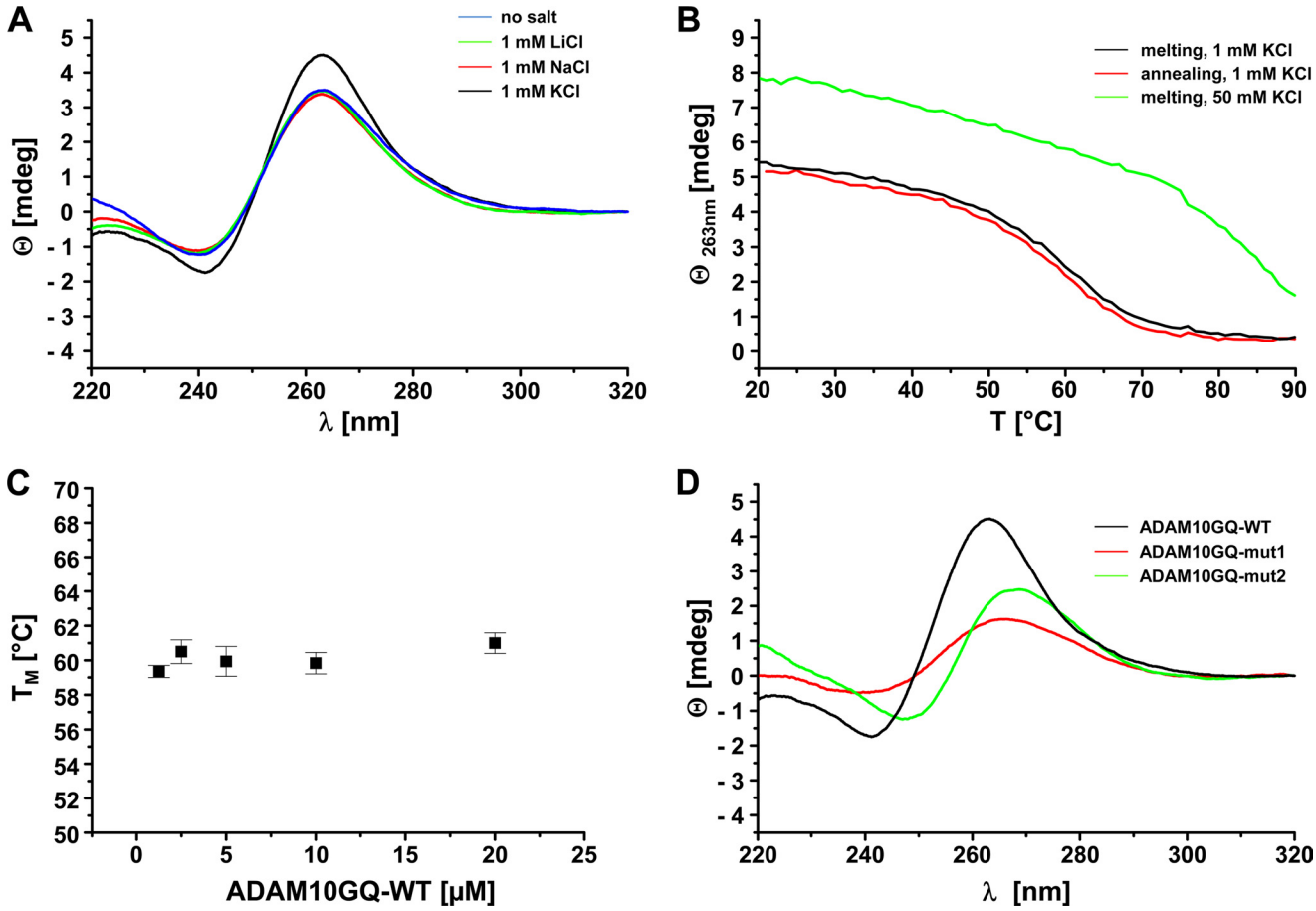

FIGURE 2. **Biophysical analysis of the ADAM10 G-quadruplex motif.** *A*, CD spectra of 5 μM ADAM10GQ-WT oligonucleotide in the absence (*blue*) or presence of different monovalent cations (*green*, LiCl; *red*, NaCl; *black*, KCl; 1 mM each) in 10 mM Tris/HCl (pH 7.4), 0.1 mM EDTA. Note that the formation of a stable G-quadruplex structure was strongly induced in the presence of 1 mM KCl. *B*, CD melting experiments of 5 μM ADAM10GQ-WT in the presence of 1 mM KCl. Melting (*black*) and annealing (*red*) curves are almost identical and show a T_m of 60 ± 1 °C. In contrast, at 50 mM KCl (*green*), the folded G-quadruplex could not be unfolded at higher temperatures. *C*, plot of T_m values for ADAM10GQ-WT at various strand concentrations. All experiments were performed in the presence of 10 mM Tris/HCl (pH 7.4), 0.1 mM EDTA, and 1 mM KCl. Results are expressed as the mean ± S.D. of at least three different measurements. *D*, CD spectra in the presence of 1 mM KCl of ADAM10GQ-WT (*black*) and mutated variants thereof (*red*, ADAM10GQ-mut1; *green*, ADAM10GQ-mut2).

between human, chimpanzee, and rhesus monkey, indicating that it might have an important physiological function. To prove that this sequence indeed forms a stable G-quadruplex secondary structure, we performed CD spectroscopy, a standard technique to investigate the formation of G-quadruplex structures by oligonucleotides (34, 50). We analyzed the CD spectrum of ADAM10GQ-WT RNA-oligonucleotide (Fig. 1*C*) at pH 7.4 in the absence of salt or in the presence of 1 mM LiCl, NaCl, or KCl (Fig. 2*A*). As a control, we determined the CD spectrum for the previously characterized G-quadruplex of N-*ras* in the presence of 1 mM and 100 mM KCl (supplemental Fig. 1) (35). We observed the characteristic CD signature for a parallel RNA G-quadruplex (51) with a positive peak at 263 nm and a negative peak at 241 nm for ADAM10GQ-WT in the absence of salt, suggesting an inherent propensity of the sequence to form a G-quadruplex (Fig. 2*A*) (35, 37). Addition of 1 mM KCl significantly increased the positive peak at 263 nm and a negative peak at 241 nm, consistent with the finding that potassium ions could stabilize the formation of G-quadruplexes (32, 34–37, 52). In the presence of 1 mM LiCl, the CD spectrum was not altered as expected because lithium ions do not support the formation of G-quadruplexes (35, 37, 52). In our experiments, addition of 1 mM NaCl also had no effect on G-quadruplex formation, possibly due to the lower propensity of sodium ions compared with potassium ions to stabilize G-quadruplex structures (32, 34, 35, 37, 42, 52).

To determine the thermal stability of the G-quadruplex, we performed CD melting experiments at 263 nm of ADAM10GQ-WT in the presence of 1 mM KCl (Fig. 2*B*). Melting and annealing curves were virtually identical and T_m was determined to be 60 ± 1 °C, assuming a single cooperative transition between the folded and unfolded state of the G-quadruplex structure (37, 45). Consistent with previous reports (35–37, 40–42, 53), at higher KCl concentrations (50 mM), the structure could not be unfolded even at 90 °C, which is indicative of a very stable G-quadruplex (Fig. 2*B*). Based on the van't Hoff method (45), we determined the thermodynamic parameters for the melting curves at 1 mM KCl. The Gibbs' free energy ΔG_{vH} at 37 °C was −10.6 ± 0.8 kJ/mol, suggesting the formation of a stable G-quadruplex structure at 37 °C. Moreover, the calculated values for ΔH_{vH} (−151.5 ± 13.2 kJ/mol) and ΔS_{vH} (−0.45 ± 0.04 kJ/mol K) were comparable with published data of other G-quadruplexes (37, 53–55). To further investigate whether ADAM10GQ-WT forms an intermolecular or intra-

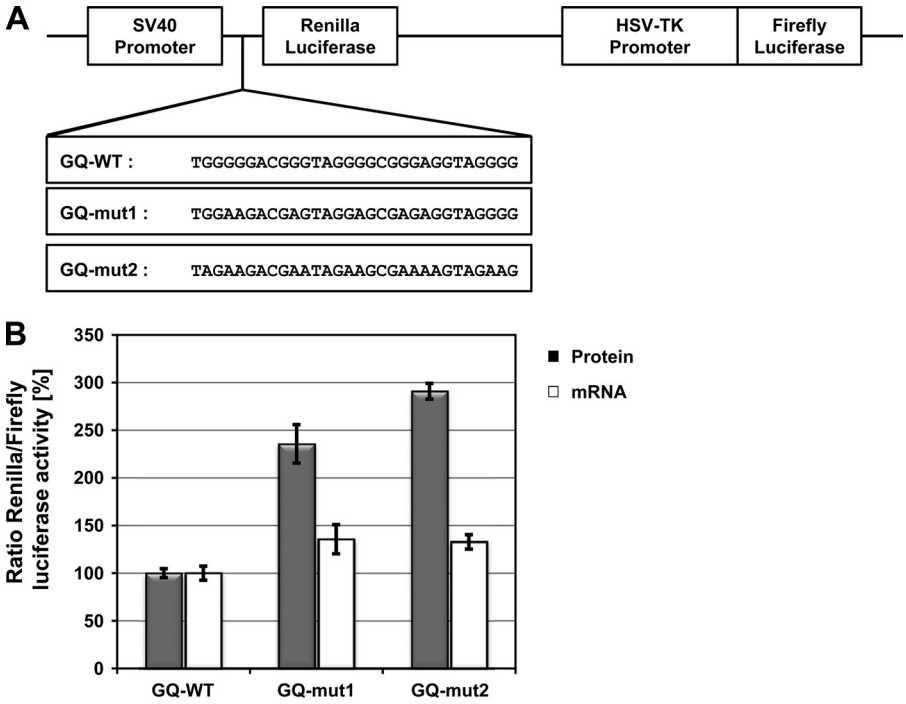

FIGURE 3. **Translational repression of a luciferase reporter by the ADAM10 G-quadruplex motif.** *A,* Schematic representation of the plasmids used for reporter gene assays. The wild-type G-quadruplex sequence (GQ-WT) of the ADAM10 5′-UTR or mutated variants thereof were cloned directly in front of the Renilla coding region. *B,* 24 h after transfection of the indicated plasmids in HEK293 cells dual-luciferase assays were performed and mRNA was isolated. Renilla luciferase activity was normalized to Firefly luciferase activity and the value for GQ-WT was set to 100%. C_T values for Renilla and Firefly luciferase mRNA were determined by quantitative RT-PCR and the ratio of C_T Renilla/C_T Firefly was calculated as described (47). Results are expressed as means ± S.D. of at least three independent experiments made in triplicates.

molecular G-quadruplex, we determined the melting temperature T_m at different concentrations of ADAM10GQ-WT in the range of 1–20 μM and in the presence of 1 mM KCl (35–37, 53, 56). As shown in Fig. 2*C*, T_m remains unchanged at 60 °C in this concentration range, indicating that ADAM10GQ-WT forms a unimolecular G-quadruplex. Finally, we performed CD spectroscopy with mutant variants of ADAM10GQ-WT. We substituted several guanines, which might be involved in G-quadruplex formation by adenines (Fig. 1*C*), to prevent the formation of an intramolecular, parallel G-quadruplex structure (35–37). Indeed, for ADAM10GQ-mut1 and ADAM10GQ-mut2, both CD spectra showed a lower ellipticity in the presence of 1 mM KCl (Fig. 2*D*). Moreover, compared with the CD spectrum of the wild-type sequence, the maxima and minima were shifted slightly to higher wave lengths similar to the CD spectra of unstructured, single-stranded RNA (37, 40, 57). Taken together, our biophysical analysis confirms that the ADAM10GQ-WT RNA forms a highly stable, unimolecular, parallel G-quadruplex near physiological pH and salt conditions.

The ADAM10 G-quadruplex Motif Inhibits Translation of a Luciferase Reporter in Vivo—Recently, it was shown that G-quadruplex motifs within 5′-UTRs inhibit translation of their downstream gene *in vitro* and *in vivo* (35–42). Moreover, artificially introduced RNA-G-quadruplex motifs near the ribosomal binding site suppress bacterial gene expression (58). Therefore, we investigated whether the *ADAM10* G-quadruplex motif could inhibit translation in living cells. We cloned the *ADAM10* G-quadruplex motif and its two mutant variants in front of the *Renilla* luciferase coding region of the psiCHECK-2 vector (Fig. 3*A*). 24 h after transfection of the resulting plasmids in HEK293 cells, we performed Dual-Luciferase reporter assays as described (36, 37, 39). Strikingly, for both mutant variants, GQ-mut1 and GQ-mut2, we observed a significant increase in *Renilla* luciferase activity normalized to firefly luciferase activity ratios (Fig. 3*B*). Using quantitative RT-PCR, we observed only a very subtle increase in mRNA levels for both mutants (Fig. 3*B*). These results confirm that the *ADAM10* G-quadruplex can suppress translation.

Inhibition of G-quadruplex Formation in the Context of the Entire ADAM10–5′-UTR Facilitates Luciferase Translation—To further demonstrate that the G-quadruplex motif is an inhibitory element within the entire context of the *ADAM10*-5′-UTR, we performed *in vitro* translation assays. Equal amounts of *in vitro*-transcribed 5′-UTR-GQ-WT-luciferase, 5′-UTR-GQ-mut1 luciferase and 5′-UTR-GQ-mut2 luciferase mRNA were translated in nuclease-treated rabbit reticulocyte lysate. Consistent with the data presented in Fig. 3*B*, luciferase activity measurements revealed that both mutations of the *ADAM10* G-quadruplex motif resulted in a 3-fold increase in firefly luciferase activity compared with the wild-type 5′-UTR-luciferase construct (Fig. 4). Taken together, these findings demonstrate that the *ADAM10* G-quadruplex alone or within the context of the *ADAM10*-5′-UTR represses translation of a reporter gene and suggests that the formation of a very stable G-quadruplex secondary structure is responsible for translational repression.

The G-quadruplex Efficiently Inhibits ADAM10 Translation—Recently, we demonstrated that the 5′-UTR of *ADAM10* is involved in translational repression of ADAM10 (18). Based on

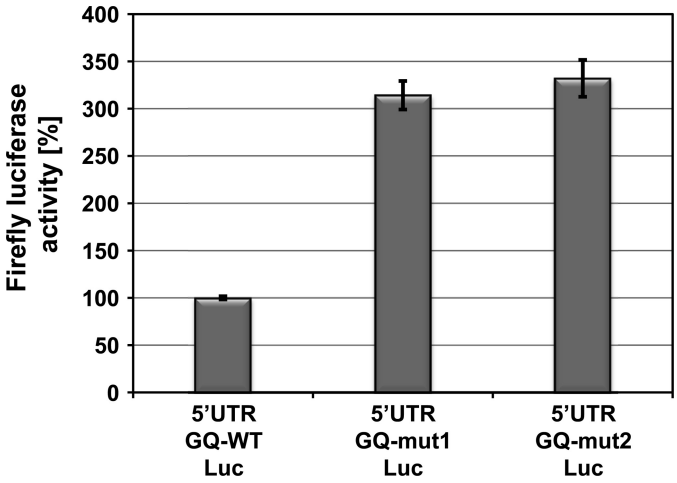

FIGURE 4. **ADAM10 G-quadruplex motif in context of entire 5′-UTR inhibits translation of firefly luciferase reporter.** Equal amounts of *in vitro*-transcribed firefly luciferase mRNAs with the full-length 5′-UTR of ADAM10 containing the wild-type G-quadruplex sequence (5′-UTR-GQ-WT-Luc) or the indicated mutations as depicted in Fig. 1*C* (5′-UTR-GQ-mut1-Luc, 5′-UTR-GQ-mut2-Luc) were subjected to *in vitro* translation using nuclease-treated rabbit reticulocyte lysates. Results are expressed as means ± S.D. of three independent experiments made in triplicate.

the *in vitro* findings, we assumed that the *ADAM10* G-quadruplex motif could contribute to this translational inhibition. To prove this, we cloned the *ADAM10* G-quadruplex motif and the corresponding mutants directly in front of the *ADAM10* coding region. After transient transfection of these cDNA constructs in HEK293 cells, we observed a 9.5- to 15-fold increase in ADAM10 protein levels when the *ADAM10* G-quadruplex motif was mutated (Fig. 5, *A* and *B*). As shown previously, overexpression of ADAM10 results predominantly in the generation of immature ADAM10 (18). Nevertheless, we detected elevated levels of secreted APPsα in supernatants of cells transfected with G-quadruplex mutations (Fig. 5, *A* and *C*). Because there was only a small increase in mRNA levels (Fig. 5*B*), our data strongly suggest that the G-quadruplex is involved in translational repression of ADAM10.

Taken together, we demonstrate that the *ADAM10*-5′-UTR contains a G-quadruplex motif that is able to form a highly stable secondary structure *in vitro*. This G-quadruplex is sufficient for translational suppression of a reporter gene and ADAM10 in living cells. Hence, the G-quadruplex secondary structure is one element contributing to the translational inhibition of ADAM10 expression via its 5′-UTR.

DISCUSSION

There is growing evidence that canonical repeats of G-rich stretches in DNA or RNA can form stable G-quadruplex secondary structures, which are implicated in a variety of biological processes like telomere protection, stabilization, and replication, as well as transcription, splicing, and translation of RNA (30, 33, 59–61). Recently, it was demonstrated that besides telomeres and promoter regions, 5′- and 3′-untranslated regions of mRNAs are hotspots of potential G-quadruplex forming sequences (30). The authors suggested that G-quadruplex structures within 3′-UTRs might facilitate transcriptional termination leading to an efficient cleavage at the polyadenylation site and polyadenylation of the mRNA (30). In addition, more recently, it was demonstrated that stable G-quadruplex secondary structures within the 3′-UTR of *PSD95* and CaM kinase IIa are important neurite mRNA-targeting elements (62). On the other hand, G-quadruplex signature motifs occur predominantly at the 5′ end of the 5′-UTR, which suggests that G-quadruplex secondary structures are involved in translational regulation either by inhibiting the formation of the initiation complex or by inhibition of the scanning ribosome (30). In agreement with this hypothesis, a series of recent reports demonstrate that the 5′-UTRs of N-*ras*, *Zic-1*, membrane-type matrix metalloproteinase 3, *ESR-1*, *Bcl-2*, and others contain a G-quadruplex motif that inhibits the translation of their downstream genes (35–42).

We recently demonstrated that the 444-nucleotide-long, GC-rich 5′-UTR of *ADAM10* is responsible for the translational repression of ADAM10 (18). Using the G-quadruplex secondary prediction algorithm Quadfinder (49), we now identified a potential G-quadruplex motif between nucleotides 66 and 94 of the human *ADAM10* 5′-UTR consistent with the transcriptome-wide prediction analysis of G-quadruplex structures reported previously (30, 40). It was reported that RNA nucleosides prefer the anti-conformation of the glycosidic bond due to the $C_{3'}$-endo puckering of sugar, and hence RNA G-quadruplex structures adopt a parallel topology with a characteristic CD spectrum (34, 51). Consistent with this finding and previously reported RNA-G-quadruplexes, our CD spectroscopy analyses provide evidence that the G-quadruplex sequence of the *ADAM10* 5′-UTR forms a parallel, intramolecular G-quadruplex secondary structure that is further stabilized by potassium ions. We demonstrate that even at 1 mM KCl, the G-quadruplex is extremely stable and has a high melting temperature of 60 ± 1 °C, whereas at 50 mM KCl, the G-quadruplex could not be unfolded even at 90 °C, arguing that under physiological conditions at 37 °C and an intracellular potassium concentration of ~130 mM, the formation of the G-quadruplex structure is favored highly. Similar results were reported for the G-quadruplex of the N-*ras* 5′-UTR and *TRF2* 5′-UTR in the presence of 1 mM KCl (35, 41) (see also supplemental Fig. 1). Moreover, determination of the thermodynamic parameters $\Delta G_{vH} = -10.6 \pm 0.8$ kJ/mol, $\Delta H_{vH} = -151.5 \pm 13.2$ kJ/mol, and $\Delta S_{vH} = -0.45 \pm 0.04$ kJ/mol K, in the presence of 1 mM KCl are comparable with known DNA and RNA G-quadruplexes (37, 54, 55). In a recent study, the dependence of the stability of RNA G-quadruplexes on the loop length between the G-quadruplex forming G-tetrads was determined (53). The authors found that the thermodynamic stability but not the structure is dependent on loop length. G-quadruplexes with long loops, *e.g.* oligonucleotides with two or four nucleotides between each G-tetrad, which were termed oligonucleotide library L222 or L444, have melting temperatures between 67 and 50 °C in the presence of 5 mM KCl (53). Our data are in accordance with these results as the *ADAM10* G-quadruplex could be grouped in the oligonucleotide library categories L222, L331, or L322 with a total loop length of six or seven nucleotides (53).

To investigate the effect of the G-quadruplex structure on translation, we performed two different well established assays (35–42): Dual-Luciferase reporter assays and *in vitro* transla-

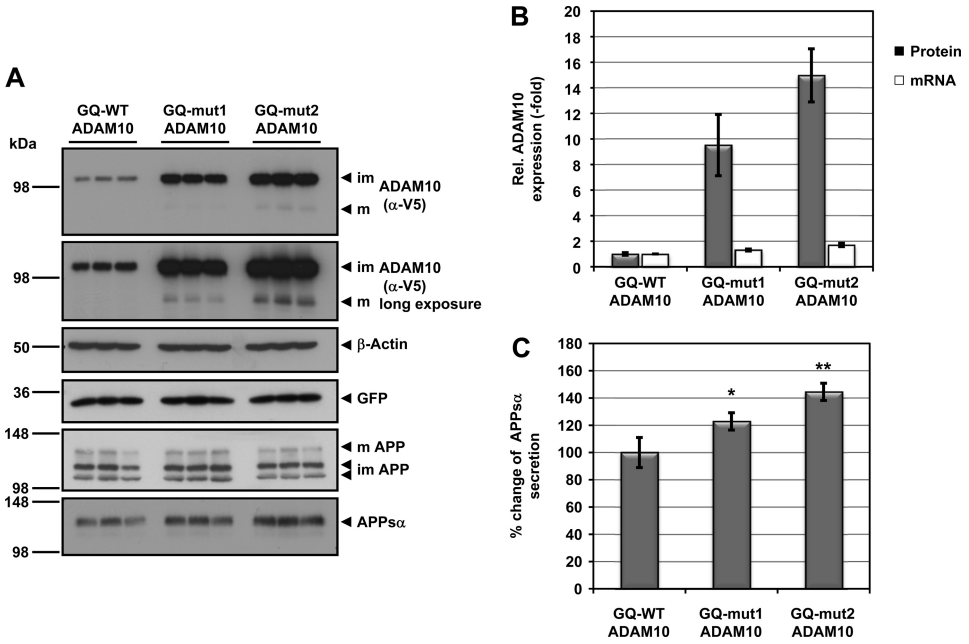

FIGURE 5. **ADAM10 expression is repressed by the G-quadruplex motif.** *A*, HEK293 cells were transiently transfected with the indicated ADAM10 cDNA constructs, and lysates were analyzed by immunoblotting for V5-tagged ADAM10, endogenous APP, β-actin as loading control, and GFP as transfection control. Supernatants were analyzed for APPsα secretion using antibody 2D8. Cellular APP is present in low molecular weight immature forms (*im*) and high molecular weight mature form (*m*). ADAM10 is present as a mature (*m*) form and predominantly as an immature (*im*) form. *B*, quantification of ADAM10 protein (*black bars*) and mRNA levels (*white bars*) from cells transfected with ADAM10 cDNA constructs shown in *A*. ADAM10 protein levels were normalized to GFP and actin levels. The signal for ADAM10 with the wild-type G-quadruplex GQ-WT ADAM10 was set to 1. Results are expressed as the means ± S.D. from three experiments made in triplicate. ADAM10 mRNA was normalized to glycerolaldehyde-3-phosphate-dehydrogenase mRNA levels, and the signal for GQ-WT ADAM10 was set to 1. Results are expressed as the means ± S.D. from three experiments. *C*, quantification of secreted APPsα from cells transfected with the indicated ADAM10 variants were shown in *A*. The signal for APPsα from GQ-WT ADAM10 transfected cells was set to 100%. Results are expressed as the means ± S.D. from three experiments. *Asterisks* indicate statistical significance (one-way analysis of variance with Dunnett's post test) relative to GQ-WT ADAM10 transfected cells (*, $p < 0.05$; **, $p < 0.01$).

tion assays with luciferase mRNAs containing the wild-type *ADAM10* 5′-UTR or *ADAM10* 5′-UTRs with a mutated G-quadruplex motif. Using CD spectroscopy, we demonstrated that our two RNA oligonucleotides with the mutated G-quadruplex sequences do not have the same characteristic CD spectrum as the wild-type oligonucleotide. Dual-Luciferase reporter assays revealed a significant increase in luciferase activity for the two mutant variants compared with the wild-type G-quadruplex-containing reporter. This increase in reporter activity is consistent with previously published reports for G-quadruplex containing 5′-UTR mRNAs such as *Zic-1* (36), membrane-type matrix metalloproteinase 3 (37), *EBAG9*, *AASDHPPT*, *BARHL2*, *THRA*, *NCAM2*, and *FDZ2* (40). To further confirm these results, we performed *in vitro* translation assays using equal amounts of *in vitro*-transcribed luciferase mRNAs containing the full-length *ADAM10* 5′-UTR with the wild-type G-quadruplex motif and mutant variants thereof. Mutation of the *ADAM10* G-quadruplex signature motif resulted in a 3-fold increase of luciferase activity for both mutants compared with the wild-type 5′-UTR. These findings are again in agreement with recently described results for the 5′-UTR mRNAs of N-*ras* (35), *ESR-1* (38), *Bcl-2* (42), and *TRF2* (41).

We further investigated the effect of the G-quadruplex and mutations thereof on the translation of ADAM10. As expected from our reporter assays, we observed that mutation of the G-quadruplex motif resulted in higher ADAM10 levels and in an increase of APPsα secretion. We observed a 9.5- to 15-fold increase in ADAM10 expression with our mutated G-quadruplex ADAM10 constructs, which is in accordance to our recently observed 9-fold increase of ADAM10 expression after transient expression of Δ1–155-5′-UTR ADAM10, a construct lacking the first 155 nucleotides of the *ADAM10* 5′-UTR and hence the entire G-quadruplex motif (18). However, deletion of the first 259 nucleotides of the *ADAM10* 5′-UTR led to a nearly 100-fold increase in expression of ADAM10 (18), strongly suggesting that the *ADAM10* 5′-UTR contains several translational inhibitory elements and that the G-quadruplex motif is one of these inhibitory elements. Although we observed a significant increase in ADAM10 protein, we only detected a 1.3- and 1.7-fold increase in ADAM10 mRNA levels for GQ-mut1-ADAM10 and GQ-mut2-ADAM10, respectively. However, such a moderate increase in mRNA levels could not explain the 9.5- and 15-fold increase of protein levels. Because DNA could also form G-quadruplex secondary structures, we could not completely rule out that transcription of *ADAM10* might be influenced by a DNA-G-quadruplex formed in the complementary strand (30, 59). In fact, it was reported that the transcription of several proto-oncogenes, including c-*myc*, K-*ras*, c-*kit*, *Bcl-2*, and platelet-derived growth factor receptor-β is suppressed by G-quadruplex structures in their promoters (63–67). Because the expression of *ADAM10* in our cDNA constructs is under the control of the very strong CMV promoter, it is rather unlikely that increased transcription is responsible for the observed effects. Instead, it was reported that the cytoplasmic 5′-3′-exoribonuclease mXrn1, which is involved in mRNA degradation, exhibits a substrate preference for G-quadruplex

containing mRNAs (68). This could explain the slight increase in mRNA levels of GQ-mut1-ADAM10 and GQ-mut2-ADAM10.

Because the G-quadruplex in the *ADAM10* 5′-UTR is involved in translational repression, it appears reasonable that genetic variations in the G-quadruplex motif might have an impact on translation of ADAM10. To identify SNPs in G-quadruplex motif containing 5′-UTRs, a bioinformatic analysis was recently performed using all human G-quadruplex sequences from the UTRef collection of the UTRdb database (40). Interestingly, in 5% of these sequences, SNPs occur, which might have an impact on translation of the downstream gene (40). However, no SNP was found for the *ADAM10* G-quadruplex sequence, which does not rule out that SNPs in other regions of the *ADAM10* 5′-UTR might have an impact on translation.

Translational repression of mRNAs is often achieved via RNA secondary structures in 5′-UTRs (19, 69, 70). Interestingly, the 5′-UTRs of the mRNAs coding for BACE1, APP, and ADAM10 were found to be involved in translational regulation of their downstream gene products (18, 71, 72). Translational repression of BACE1 is mediated by its long, structured, and upstream ORFs containing 5′-UTR (22–24). Energy deprivation results in phosphorylation of eIF2α and consequently in an arrest of global translation; however, *BACE1* expression is increased due to reinitiation of translation at the initiation codon of the *BACE1* mRNA (25, 73). In contrast, it was reported that similar to the 5′-UTR of L- and H-ferritin the 5′-UTR of APP contains an IRE, and translation of APP was repressed by IRP1 under low cellular iron concentrations (74). Iron uptake in cells result in the dissociation of the IRE-IRP repressor complex and increased translation of ferritin and APP (72). The exact mechanism how this is accomplished is not known yet; however, a recent study suggests that Fe^{2+} might weaken the IRE-IRP repressor complex *in vitro* (75). Moreover, it was reported that binding of poly-C binding protein 1 to the acute box cis element within the 5′-UTR of the human H-ferritin mRNA facilitates H-ferritin translation when the cytosolic iron concentration is increased (76). These data demonstrate that translational inhibitory RNA elements could be modulated by RNA binding proteins. Therefore, we hypothesize that such RNA binding proteins selectively bind and modulate the *ADAM10* 5′-UTR G-quadruplex structure. FMRP, an RNA binding protein involved in mRNA translation, splicing, and mRNA transport in the cell, was identified as a G-quadruplex interacting protein (77–79). FMRP binds tightly to G-quadruplexes in the 5′-UTRs of protein phosphatase 2A catalytic subunit and *MAP1B* (microtubule-associated protein 1B), and it was suggested that this interaction represses translation of both mRNAs (77, 80). Furthermore, it was demonstrated that the FMRP-G-quadruplex repressor in the *MAP1B* 5′-UTR was destabilized by an increased FMRP concentration, suggesting that the variation of FMRP concentration in response to neuronal stimulation might act as a regulatory switch from translational repressor to a translational activator (43). The RGG box of FMRP was shown to be responsible for the interaction with the G-quadruplex secondary structure in the *MAP1B* 5′-UTR (43). Therefore, methylation of RGG motifs in FMRP by PMRT1 might regulate the interaction of FMRP with polyribosomes and G-quadruplex-containing mRNAs (81). In addition, members of the hnRNP A family were reported to destabilize G-quadruplex structures by a so-far unknown mechanism (44, 82). Apart from FMRP and hnRNP A, there are several proteins described that are able to interact and modify G-quadruplex structures in DNA and RNA substrates. For instance, specific RNA and DNA helicases are able to unwind G-quadruplex structures (83–86). Deficiencies of certain G-quadruplex resolving helicases result in abnormal mRNA deadenylation and decay and in perturbed telomere maintenance and cellular DNA replication, leading to cancer (87). In addition, it was reported recently that nucleolin stabilizes the G-quadruplex within the c-*myc* promoter and inhibits transcription (88). Interestingly, nucleolin interacts with G-rich sequences in UTRs or the coding region of a lot of mRNAs and was found to enhance their translation (89), suggesting that nucleolin might function as a RNA-G-quadruplex interacting factor.

ADAM10 expression and activity is reduced in platelets and neurons of Alzheimer disease patients (90, 91). Translational repression of ADAM10 might be one possible explanation for this observation. Based on the above discussed regulatory mechanisms, we are currently investigating whether ADAM10 translation is modulated by G-quadruplex interacting proteins.

Taken together, we provide evidence that a stable G-quadruplex secondary structure within the *ADAM10* 5′-UTR is involved in translational regulation of ADAM10. The development of selective G-quadruplex unwinding molecules, which are able to cross the blood brain barrier, might be a new therapeutic venue for the treatment of Alzheimer disease.

Acknowledgment—We thank Mehak Mumtaz, a scholar of the Amgen Summer School Programme, for technical assistance.

REFERENCES

1. Haass, C., and Selkoe, D. J. (2007) *Nat. Rev. Mol. Cell Biol.* **8,** 101–112
2. Meziane, H., Dodart, J. C., Mathis, C., Little, S., Clemens, J., Paul, S. M., and Ungerer, A. (1998) *Proc. Natl. Acad. Sci. U.S.A.* **95,** 12683–12688
3. Furukawa, K., Sopher, B. L., Rydel, R. E., Begley, J. G., Pham, D. G., Martin, G. M., Fox, M., and Mattson, M. P. (1996) *J. Neurochem.* **67,** 1882–1896
4. Haass, C., Hung, A. Y., Schlossmacher, M. G., Teplow, D. B., and Selkoe, D. J. (1993) *J. Biol. Chem.* **268,** 3021–3024
5. Koike, H., Tomioka, S., Sorimachi, H., Saido, T. C., Maruyama, K., Okuyama, A., Fujisawa-Sehara, A., Ohno, S., Suzuki, K., and Ishiura, S. (1999) *Biochem. J.* **343,** 371–375
6. Buxbaum, J. D., Liu, K. N., Luo, Y., Slack, J. L., Stocking, K. L., Peschon, J. J., Johnson, R. S., Castner, B. J., Cerretti, D. P., and Black, R. A. (1998) *J. Biol. Chem.* **273,** 27765–27767
7. Lammich, S., Kojro, E., Postina, R., Gilbert, S., Pfeiffer, R., Jasionowski, M., Haass, C., and Fahrenholz, F. (1999) *Proc. Natl. Acad. Sci. U.S.A.* **96,** 3922–3927
8. Postina, R., Schroeder, A., Dewachter, I., Bohl, J., Schmitt, U., Kojro, E., Prinzen, C., Endres, K., Hiemke, C., Blessing, M., Flamez, P., Dequenne, A., Godaux, E., van Leuven, F., and Fahrenholz, F. (2004) *J. Clin. Invest.* **113,** 1456–1464
9. Kuhn, P. H., Wang, H., Dislich, B., Colombo, A., Zeitschel, U., Ellwart, J. W., Kremmer, E., Rossner, S., and Lichtenthaler, S. F. (2010) *EMBO J.* **29,** 3020–3032
10. Hartmann, D., de Strooper, B., Serneels, L., Craessaerts, K., Herreman, A., Annaert, W., Umans, L., Lübke, T., Lena Illert, A., von Figura, K., and Saftig, P. (2002) *Hum. Mol. Gen.* **11,** 2615–2624
11. Jorissen, E., Prox, J., Bernreuther, C., Weber, S., Schwanbeck, R., Serneels,

L., Snellinx, A., Craessaerts, K., Thathiah, A., Tesseur, I., Bartsch, U., Weskamp, G., Blobel, C. P., Glatzel, M., De Strooper, B., and Saftig, P. (2010) *J. Neurosci.* **30,** 4833–4844
12. Yang, P., Baker, K. A., and Hagg, T. (2006) *Prog. Neurobiol.* **79,** 73–94
13. Pruessmeyer, J., and Ludwig, A. (2009) *Semin. Cell Dev. Biol.* **20,** 164–174
14. Anders, A., Gilbert, S., Garten, W., Postina, R., and Fahrenholz, F. (2001) *FASEB J.* **15,** 1837–1839
15. Moss, M. L., Bomar, M., Liu, Q., Sage, H., Dempsey, P., Lenhart, P. M., Gillispie, P. A., Stoeck, A., Wildeboer, D., Bartsch, J. W., Palmisano, R., and Zhou, P. (2007) *J. Biol. Chem.* **282,** 35712–35721
16. Tippmann, F., Hundt, J., Schneider, A., Endres, K., and Fahrenholz, F. (2009) *FASEB J.* **23,** 1643–1654
17. Donmez, G., Wang, D., Cohen, D. E., and Guarente, L. (2010) *Cell* **142,** 320–332
18. Lammich, S., Buell, D., Zilow, S., Ludwig, A. K., Nuscher, B., Lichtenthaler, S. F., Prinzen, C., Fahrenholz, F., and Haass, C. (2010) *J. Biol. Chem.* **285,** 15753–15760
19. Gebauer, F., and Hentze, M. W. (2004) *Nat. Rev. Mol. Cell Biol.* **5,** 827–835
20. Jackson, R. J., Hellen, C. U., and Pestova, T. V. (2010) *Nat. Rev. Mol. Cell Biol.* **11,** 113–127
21. Sonenberg, N., and Hinnebusch, A. G. (2009) *Cell* **136,** 731–745
22. De Pietri Tonelli, D., Mihailovich, M., Di Cesare, A., Codazzi, F., Grohovaz, F., and Zacchetti, D. (2004) *Nucleic Acids Res.* **32,** 1808–1817
23. Lammich, S., Schöbel, S., Zimmer, A. K., Lichtenthaler, S. F., and Haass, C. (2004) *EMBO Rep.* **5,** 620–625
24. Rogers, G. W., Jr., Edelman, G. M., and Mauro, V. P. (2004) *Proc. Natl. Acad. Sci. U.S.A.* **101,** 2794–2799
25. O'Connor, T., Sadleir, K. R., Maus, E., Velliquette, R. A., Zhao, J., Cole, S. L., Eimer, W. A., Hitt, B., Bembinster, L. A., Lammich, S., Lichtenthaler, S. F., Hébert, S. S., De Strooper, B., Haass, C., Bennett, D. A., and Vassar, R. (2008) *Neuron* **60,** 988–1009
26. Hinnebusch, A. G. (1997) *J. Biol. Chem.* **272,** 21661–21664
27. Vattem, K. M., and Wek, R. C. (2004) *Proc. Natl. Acad. Sci. U.S.A.* **101,** 11269–11274
28. Muckenthaler, M., Gray, N. K., and Hentze, M. W. (1998) *Mol. Cell* **2,** 383–388
29. Hentze, M. W., Muckenthaler, M. U., Galy, B., and Camaschella, C. (2010) *Cell* **142,** 24–38
30. Huppert, J. L., Bugaut, A., Kumari, S., and Balasubramanian, S. (2008) *Nucleic Acids Res.* **36,** 6260–6268
31. Huppert, J. L. (2010) *FEBS J.* **277,** 3452–3458
32. Burge, S., Parkinson, G. N., Hazel, P., Todd, A. K., and Neidle, S. (2006) *Nucleic Acids Res.* **34,** 5402–5415
33. Patel, D. J., Phan, A. T., and Kuryavyi, V. (2007) *Nucleic Acids Res.* **35,** 7429–7455
34. Paramasivan, S., Rujan, I., and Bolton, P. H. (2007) *Methods* **43,** 324–331
35. Kumari, S., Bugaut, A., Huppert, J. L., and Balasubramanian, S. (2007) *Nat. Chem. Biol.* **3,** 218–221
36. Arora, A., Dutkiewicz, M., Scaria, V., Hariharan, M., Maiti, S., and Kurreck, J. (2008) *RNA* **14,** 1290–1296
37. Morris, M. J., and Basu, S. (2009) *Biochemistry* **48,** 5313–5319
38. Balkwill, G. D., Derecka, K., Garner, T. P., Hodgman, C., Flint, A. P., and Searle, M. S. (2009) *Biochemistry* **48,** 11487–11495
39. Halder, K., Wieland, M., and Hartig, J. S. (2009) *Nucleic Acids Res.* **37,** 6811–6817
40. Beaudoin, J. D., and Perreault, J. P. (2010) *Nucleic Acids Res.* **38,** 7022–7036
41. Gomez, D., Guédin, A., Mergny, J. L., Salles, B., Riou, J. F., Teulade-Fichou, M. P., and Calsou, P. (2010) *Nucleic Acids Res.* **38,** 7187–7198
42. Shahid, R., Bugaut, A., and Balasubramanian, S. (2010) *Biochemistry* **49,** 8300–8306
43. Menon, L., Mader, S. A., and Mihailescu, M. R. (2008) *RNA* **14,** 1644–1655
44. Khateb, S., Weisman-Shomer, P., Hershco-Shani, I., Ludwig, A. L., and Fry, M. (2007) *Nucleic Acids Res.* **35,** 5775–5788
45. Mergny, J. L., and Lacroix, L. (2003) *Oligonucleotides* **13,** 515–537
46. Shirotani, K., Tomioka, M., Kremmer, E., Haass, C., and Steiner, H. (2007) *Neurobiol. Dis.* **27,** 102–107
47. Pfaffl, M. W. (2001) *Nucleic Acids Res.* **29,** e45
48. Kumari, S., Bugaut, A., and Balasubramanian, S. (2008) *Biochemistry* **47,** 12664–12669
49. Scaria, V., Hariharan, M., Arora, A., and Maiti, S. (2006) *Nucleic Acids Res.* **34,** W683–685
50. Balagurumoorthy, P., Brahmachari, S. K., Mohanty, D., Bansal, M., and Sasisekharan, V. (1992) *Nucleic Acids Res.* **20,** 4061–4067
51. Tang, C. F., and Shafer, R. H. (2006) *J. Am. Chem. Soc.* **128,** 5966–5973
52. Hardin, C. C., Watson, T., Corregan, M., and Bailey, C. (1992) *Biochemistry* **31,** 833–841
53. Zhang, A. Y., Bugaut, A., and Balasubramanian, S. (2011) *Biochemistry* **50,** 7251–7258
54. Rachwal, P. A., Brown, T., and Fox, K. R. (2007) *Biochemistry* **46,** 3036–3044
55. Rachwal, P. A., Brown, T., and Fox, K. R. (2007) *FEBS Lett.* **581,** 1657–1660
56. Zhang, D. H., Fujimoto, T., Saxena, S., Yu, H. Q., Miyoshi, D., and Sugimoto, N. (2010) *Biochemistry* **49,** 4554–4563
57. Gray, D. M., Liu, J. J., Ratliff, R. L., and Allen, F. S. (1981) *Biopolymers* **20,** 1337–1382
58. Wieland, M., and Hartig, J. S. (2007) *Chem. Biol.* **14,** 757–763
59. Huppert, J. L., and Balasubramanian, S. (2007) *Nucleic Acids Res.* **35,** 406–413
60. Kostadinov, R., Malhotra, N., Viotti, M., Shine, R., D'Antonio, L., and Bagga, P. (2006) *Nucleic Acids Res.* **34,** D119–124
61. Brooks, T. A., Kendrick, S., and Hurley, L. (2010) *FEBS J.* **277,** 3459–3469
62. Subramanian, M., Rage, F., Tabet, R., Flatter, E., Mandel, J. L., and Moine, H. (2011) *EMBO Rep.* **12,** 697–704
63. Siddiqui-Jain, A., Grand, C. L., Bearss, D. J., and Hurley, L. H. (2002) *Proc. Natl. Acad. Sci. U.S.A.* **99,** 11593–11598
64. Cogoi, S., and Xodo, L. E. (2006) *Nucleic Acids Res.* **34,** 2536–2549
65. Fernando, H., Reszka, A. P., Huppert, J., Ladame, S., Rankin, S., Venkitaraman, A. R., Neidle, S., and Balasubramanian, S. (2006) *Biochemistry* **45,** 7854–7860
66. Dai, J., Chen, D., Jones, R. A., Hurley, L. H., and Yang, D. (2006) *Nucleic Acids Res.* **34,** 5133–5144
67. Qin, Y., Fortin, J. S., Tye, D., Gleason-Guzman, M., Brooks, T. A., and Hurley, L. H. (2010) *Biochemistry* **49,** 4208–4219
68. Bashkirov, V. I., Scherthan, H., Solinger, J. A., Buerstedde, J. M., and Heyer, W. D. (1997) *J. Cell Biol.* **136,** 761–773
69. Pickering, B. M., and Willis, A. E. (2005) *Semin. Cell Dev. Biol.* **16,** 39–47
70. van der Velden, A. W., and Thomas, A. A. (1999) *Int. J. Biochem. Cell Biol.* **31,** 87–106
71. Willem, M., Lammich, S., and Haass, C. (2009) *Semin. Cell Dev. Biol.* **20,** 175–182
72. Cahill, C. M., Lahiri, D. K., Huang, X., and Rogers, J. T. (2009) *Biochim. Biophys. Acta* **1790,** 615–628
73. Velliquette, R. A., O'Connor, T., and Vassar, R. (2005) *J. Neurosci.* **25,** 10874–10883
74. Cho, H. H., Cahill, C. M., Vanderburg, C. R., Scherzer, C. R., Wang, B., Huang, X., and Rogers, J. T. (2010) *J. Biol. Chem.* **285,** 31217–31232
75. Khan, M. A., Walden, W. E., Goss, D. J., and Theil, E. C. (2009) *J. Biol. Chem.* **284,** 30122–30128
76. Thomson, A. M., Cahill, C. M., Cho, H. H., Kassachau, K. D., Epis, M. R., Bridges, K. R., Leedman, P. J., and Rogers, J. T. (2005) *J. Biol. Chem.* **280,** 30032–30045
77. Darnell, J. C., Jensen, K. B., Jin, P., Brown, V., Warren, S. T., and Darnell, R. B. (2001) *Cell* **107,** 489–499
78. Schaeffer, C., Bardoni, B., Mandel, J. L., Ehresmann, B., Ehresmann, C., and Moine, H. (2001) *EMBO J.* **20,** 4803–4813
79. Melko, M., and Bardoni, B. (2010) *Biochimie* **92,** 919–926
80. Castets, M., Schaeffer, C., Bechara, E., Schenck, A., Khandjian, E. W., Luche, S., Moine, H., Rabilloud, T., Mandel, J. L., and Bardoni, B. (2005) *Hum. Mol. Genet.* **14,** 835–844
81. Blackwell, E., Zhang, X., and Ceman, S. (2010) *Hum. Mol. Genet.* **19,** 1314–1323
82. Khateb, S., Weisman-Shomer, P., Hershco, I., Loeb, L. A., and Fry, M. (2004) *Nucleic Acids Res.* **32,** 4145–4154
83. Chakraborty, P., and Grosse, F. (2011) *DNA Repair* **10,** 654–665
84. Lattmann, S., Giri, B., Vaughn, J. P., Akman, S. A., and Nagamine, Y. (2010)

Nucleic Acids Res. **38,** 6219–6233
85. Creacy, S. D., Routh, E. D., Iwamoto, F., Nagamine, Y., Akman, S. A., and Vaughn, J. P. (2008) *J. Biol. Chem.* **283,** 34626–34634
86. London, T. B., Barber, L. J., Mosedale, G., Kelly, G. P., Balasubramanian, S., Hickson, I. D., Boulton, S. J., and Hiom, K. (2008) *J. Biol. Chem.* **283,** 36132–36139
87. Wu, Y., and Brosh, R. M., Jr. (2010) *FEBS J.* **277,** 3470–3488
88. González, V., Guo, K., Hurley, L., and Sun, D. (2009) *J. Biol. Chem.* **284,** 23622–23635
89. Abdelmohsen, K., Tominaga, K., Lee, E. K., Srikantan, S., Kang, M. J., Kim, M. M., Selimyan, R., Martindale, J. L., Yang, X., Carrier, F., Zhan, M., Becker, K. G., and Gorospe, M. (2011) *Nucleic Acids Res.* **39,** 8513–8530
90. Colciaghi, F., Borroni, B., Pastorino, L., Marcello, E., Zimmermann, M., Cattabeni, F., Padovani, A., and Di Luca, M. (2002) *Mol. Med.* **8,** 67–74
91. Bernstein, H. G., Bukowska, A., Krell, D., Bogerts, B., Ansorge, S., and Lendeckel, U. (2003) *J. Neurocytol.* **32,** 153–160